



AENSI Journals

Australian Journal of Basic and Applied Sciences

ISSN:1991-8178

Journal home page: www.ajbasweb.com



Steg analysis Algorithm for Edge Adaptive Least Significant Bit Matching Revisited Detection

Khalid Edris, Mohammed Adam Ibrahim Fakhreldin, Jasni Mohamad Zain, Tuty Asmawaty Abdul Kadir, Khalid Adam

University Malaysia Pahang, Faculty of Computer Systems and Software Engineering, Box. 26300. Kuantan. Malaysia

ARTICLE INFO

Article history:

Received 19 September 2014

Received in revised form

19 November 2014

Accepted 29 November 2014

Available online 27 December 2014

Keywords:

ABSTRACT

Background: Spatial domain Steganalysis technology based on digital grayscale images has drawn a lot of interest in recent years. Edge Adaptive LSB Matching Revisited (EALMR) steganography algorithm is high safety spatial domain information hiding technique which can choose embedding area based on the image context. **Objective:** This paper proposes Edge Adaptive Steganalysis algorithm based on histograms of the absolute difference of adjacent pixels to detect EALMR. **Results:** The results show that the proposed analytical algorithm based on histogram of absolute difference of adjacent pixels can effectively detect EALMR. **Conclusion:** The performance of the proposed steganalysis algorithm is better than previous algorithms in detecting of EALMR.

© 2014 AENSI Publisher All rights reserved.

To Cite This Article: Khalid Edris, Mohammed Adam Ibrahim Fakhreldin, Jasni Mohamad Zain, Tuty Asmawaty Abdul Kadir, Khalid Adam, Steg analysis Algorithm for Edge Adaptive Least Significant Bit Matching Revisited Detection. *Aust. J. Basic & Appl. Sci.*, 8(18): 617-628, 2014

INTRODUCTION

Steganography technology is an important branch in the field of information security, and its main purpose is to hide the secret to be transmitted in the carrier object with some technical means and not arouse the suspicions of the third party. The carrier for the secret information has a variety of forms, such as digital image, video, audio, and text files. Steganalysis technology is the opposite of Steganography technology, and its main purpose is to detect whether secret information is hidden in the carrier file. Steganography technology and Steganalysis technology are unity of opposites, contradictory and dependent on each other. With the increasingly widely application of information security technology, steganography technology and Steganalysis technology have enjoyed fast growth. In the field of information hiding, the digital image in spatial domain is easy to operate, can be embedded with large capacity and can be applied widely; Steganography technology and Steganalysis technology which are based on the technology of digital image spatial domain secret and hidden analysis technology receive rapid development.

Least Significant Bit (LSB) Replacement (Chandramouli *et al.*, 2003) is the earliest spatial domain Steganography technology, and reaches the purpose of embedding secret information by directly reversing the lowest significance bit of grayscale value which is different from the secret information bit value (Bender *et al.*, 1996). But this change will bring image pixel gray value histogram obvious "value effect", so the LSB replacement of algorithm secret will soon be breached, Steganalysis algorithm such as Chi - square (Westfeld and Pfitzmann, 2000) and (Fridrich *et al.*, 2001; Fridrich and Goljan 2002) RS detection, WS test (Schottle *et al.*, 2012) and AUMP test (Fillatre, 2012), etc. can effectively detect LSB replacement hiding algorithm. Compared to the LSB hiding algorithm, LSB matching (Least Significant Bit Matching) (Sharp, 2001) hiding algorithm has a qualitative change. LSB matching algorithm was not regularly on the lowest effective pixels directly, but a plus or minus 1 at random. This kind of operation avoids the "value effect" in the LSB replacement algorithm. But LSB matching algorithm has its own weaknesses, the algorithm embedded mechanism destroys the natural images of smooth area of the correlation of adjacent pixels, making the adjacent pixels have the characteristics of independence, which is impossible in the smooth area of the original natural images, and thus the LSB matching algorithm is also be breached by a variety of hidden analysis algorithm (Harmsen and Pearlman, 2003; Cancelli *et al.*, 2008; Goljan *et al.*, 2006; Ker, 2005). LSB matching revisited (LSBMR) [1] uses a pair of pixels as an embedding unit, in which the LSB of the first pixel carries one bit of secret message, and the relationship

Corresponding Author: Khalid Edris, University Malaysia Pahang, Faculty of Computer System and Software Engineering, Box.26300. Lebuhraya TunRazak, Gambang, Kuantan, Pahang Darul Makmur, Kuantan. Malaysia.
E-mail: khalod07@yahoo.com

of the two pixel values carries another bit of secret message. Luo *et al.*, (2010) presented a new spatial domain LSB matching steganography algorithm (Edge Adaptive LSB Matching Revisited, referred EALMR). EALMR steganography algorithm is high safety spatial domain information hiding techniques which can choose embedding area based on the image context. Embedding area by choosing the area with rich texture can reduce the change of statistical features brought by the information embedding message process. This adaptive advantage of EALMR can make it has stronger security. HUGO (Pevny *et al.*, 2010) is by far the most secure coding techniques based on steganography algorithm, its security comes from the self-adaptive mechanism of embedding information. When use HUGO algorithm to embed information, STC (Syndrome-Trellis Codes) (Filler *et al.*, 2010; Filler *et al.*, 2011) is applied, the best embedding path can be found by calculating the embedding distortion in order to minimize the effects brought by embedment of information. Also, it can also effectively avoid the wet points in wet paper coding. Currently, there are no analysis algorithms to detect EA algorithm and HUGO algorithm, but relevant research work has been made some meaningful progress (Fridrich *et al.*, 2011; Fridrich *et al.*, 2011; Gul and Kurugollu, 2011).

In the areas of steganalysis techniques, as for the features of spatial domain steganography algorithm, many algorithms are proposed to detect Steganography algorithms. Harmsen and Pearlman proposed a histogram characteristic function centroid (Histogram Characteristic Function-Center of Mass, HCF-COM) Steganalysis algorithm method (Harmsen and Pearlman, 2003). In this algorithm, histogram characteristic function is the Discrete Fourier Transform of histogram image. It can detect by comparing HCF-COM of images and calibrated images. But as the different carrier images' HCF-COM vary, sometimes even more than the difference brought by the secret information embedding process. As a result, directly comparison of HCF-COM to judge whether the image has the information hiding dose not perform well. Goljan *et al.*, (2006) proposed Wavelet Absolute Moment (WAM) Steganalysis algorithm method. Firstly, it moves the Gaussian noise to increase the signal to noise ratio, then it extracts noise component of small wave area of secret images as the features for analyzing secrets. Suppose the original image is non-stationary Gaussian signal, the noise is the smooth Gaussian signal with known variance, the secret image can be the sum of both. When image information is hidden by the LSBM algorithm, its local minimum value of the histogram increases and the local maxima value decreases. Based on this principle, Zhang *et al.*, (2007) proposed to use the sum of Amplitude of Histogram Local Extrema as the features for analyzing secrets. However, the algorithm does not consider the case of the boundary points in the histogram, when the gray value is 0, 1 only can be changed to 1, when the gray value is 255, and it can be changed to 254. Based on this, Cancem *et al.* improved the ALE analysis algorithm (Cancelli *et al.*, 2008) and consider individually the boundary points [1,2,253,254]; two-dimensional histogram local extrema amplitude characteristics is added on the original base. The sum of diagonal elements of two-dimensional histogram is added as the features. Pevny *et al.*, (2009) proposed Subtractive Pixel Adjacency Model (SPAM) Steganalysis algorithm method. It calculates the eight directions of absolute difference of horizontal, vertical, main diagonal and sub diagonal directions in the grayscale matrix. Then use Markov to build models for these grayscale matrixes. They use one-step and two -step transition probability matrix as the features for analyzing secrets. At the same time, by setting an appropriate threshold to reduce the feature dimension, the computational complexity becomes more reasonable. Fridrich and Kodovsky, (2012) proposed a rich model airspace steganalysis algorithm method. This algorithm extracts various characteristics from the airspace and forms a plurality of feature subset. These features set contain all the features, which are useful for the analysis of airspace. Various steganalysis algorithm method can achieve very good results in the detection of LSB replacement and LSB Matching algorithms, but they cannot detect EALMR algorithm and HUGO algorithm.

The rest of this paper is organized as follows: the first section explains materials and methods, which contains Edge Adaptive LSB Matching Revisited algorithm and the proposed algorithm. The second section explains results and discussion. The final section concludes the paper.

MATERIALS AND METHODS

A. Edge Adaptive LSB Matching Revisited:

In digital gray-level image, the absolute difference of pixel couple (x_i, x_{i+1}) is indicated as:

$$d = |x_{i+1} - x_i| \quad (1)$$

It is hereby to restate Information Embedding Mechanism and Data Readjusting Mechanism in EALMR:

A. Information Embedding Mechanism:

For the pixel couples in V Set $EU(t) = \{(x_i, x_{i+1}) \mid |x_i - x_{i+1}| \geq t, \forall (x_i, x_{i+1}) \in V\}$ that conforms to embedding conditions, the information will be embedded in couples according to traversal order determined by Secret Key 2 and each couple of U elements will hide 2 bits of secret information. According to relational difference between pixel value and secret information, the specific embedding mechanism can be divided into 4 cases, as follows:

Case #1: $LSB(x_i)=m_i \& f(x_i, x_{i+1})=m_{i+1}$

$$(x'_i, x'_{i+1})=(x_i, x_{i+1})$$

Case #2: $LSB(x_i)=m_i \& f(x_i, x_{i+1}) \neq m_{i+1}$

$$(x'_i, x'_{i+1})=(x_i, x_{i+1} + r)$$

Case #3 $LSB(x_i) \neq m_i \& f(x_i - 1, x_{i+1})=m_{i+1}$

$$(x'_i, x'_{i+1})=(x_i - 1, x_{i+1})$$

Case #4 $LSB(x_i) \neq m_i \& f(x_i - 1, x_{i+1}) \neq m_{i+1}$

$$(x'_i, x'_{i+1})=(x_i + 1, x_{i+1}) \quad (2)$$

In these formulas, m_i and m_{i+1} refer to secret information to be embedded into the pixel couple (x_i, x_{i+1}) , and (x'_i, x'_{i+1}) refers to secret-held pixel couple after the secret information is embedded; r random refers to +1 or -1, and the $f(a, b)$ is defined as follows:

$$f(a, b) = LSB\left(\left\lfloor \frac{a}{2} \right\rfloor + b\right)$$

A.ii Data Readjusting Mechanism:

If the secret-held pixel couple (x'_i, x'_{i+1}) does not conform to $|x'_{i+1} - x'_i| \geq T$, or x'_i and x'_{i+1} go beyond $[0, 255]$, it is required to apply Data Readjusting Mechanism in the following readjusting formula:

$$(x''_i, x''_{i+1}) = \operatorname{argmin}_{(e_1, e_2)} \{ |e_1 - x_i| + |e_2 - x_{i+1}| \mid e_1 = x'_i + 4k_1, e_2 = x'_{i+1} + 2k_2, |e_1 - e_2| \geq T, 0 \leq e_1, e_2 \leq 255, 0 \leq T \leq 31, k_1, k_2 \in \mathbb{Z} \} \quad (3)$$

As readjusted in the formula above, $0 \leq x''_i, x''_{i+1} \leq 255$ and $|x''_i - x''_{i+1}| \geq T$ can be ensured.

B. Proposed Algorithm:

In embedding mechanism, it is assumed that four embedding cases respectively occur at the same probability of 0.25. In Case #1, the pixel couple is not changed, so the absolute difference of pixel couple after information embedding will not be changed. For such other three cases as Case #2, Case #3 and Case #4, the probability of pixel couple resulted after information embedding, that conforms to $|x'_i - x'_{i+1}| = T - 1$ or $|x'_i - x'_{i+1}| = T + 1$, is 0.5. Therefore, the probability of absolute difference of pixel couple, after information embedding, that changes from T to $T-1$ or $T+1$, is $0.75 \times 0.5 = 0.375$. If the pixel couple resulted after first information embedding conforms to $|x'_i - x'_{i+1}| < T$ the data readjusting mechanism will apply, so the pixel couple whose absolute difference changes to $T-1$ will be subject to data readjusting mechanism. It is further analyzed that when the pixel couple is selected for information embedding the precondition of the $|x_i - x_{i+1}| \geq T$ is required to be met and that each pixel couple in EALMR has at most one pixel to be added or reduced by 1, so the $|x'_i - x'_{i+1}| < T$ only occurs under the condition of $|x_i - x_{i+1}| = T$ and $|x'_i - x'_{i+1}| = T - 1$. However, $|x'_i - x'_{i+1}| = T - 1$ has four cases, including two cases for $x'_i - x'_{i+1} = T - 1$ and two cases for $x'_{i+1} - x'_i = T - 1$:

- (1) When $x'_i - x'_{i+1} = T - 1$ and $x'_{i+1} \geq 2$, after data readjusting, the case is $k_1 = 0$ and $k_2 = -1$;
- (2) When $x'_i - x'_{i+1} = T - 1$ and $0 \leq x'_{i+1} < 2$, the case is $k_1 = 1$ and $k_2 = 0$;
- (3) When $x'_{i+1} - x'_i = T - 1$ and $x'_{i+1} \leq 253$, after data readjusting, the case is $k_1 = 0$ and $k_2 = 1$;
- (4) When $x'_{i+1} - x'_i = T - 1$ and $253 < x'_{i+1} \leq 255$, the case is $k_1 = -1$ and $k_2 = 0$;

When the data readjusting mechanism is adopted, k_1 and k_2 under the influence of formula (3), will be further limited by the extraction formula of secret information in the algorithm. In EALMR, the extraction principle of secret-information

$$m_i = LSB(x''_i), m_{i+1} = f(x''_i, x''_{i+1}) = LSB\left(\left\lfloor \frac{x''_i}{2} \right\rfloor + x''_{i+1}\right), \text{ So, the formula should be adjusted by } e_1 = x'_i + 4k_1, e_2 = x'_{i+1} + 2k_2, k_1, k_2 \in \mathbb{Z}. \text{ From the four cases of embedding mechanism, } x'_i - x'_{i+1} = T - 1 \text{ only occurs under Case \#1, Case \#2 and Case \#3. It is assumed that } x'_i = x_i + r_1, x'_{i+1} = x_{i+1} + r_2, x''_i = x'_i + 4k_1, x''_{i+1} = x'_{i+1} + 2k_2. \text{ Therefore, the } |e_1 - x_i| + |e_2 - x_{i+1}| \text{ in the data readjusting mechanism can be represented by the following:}$$

$$|e_1 - x_i| + |e_2 - x_{i+1}| = |x''_i - x_i| + |x''_{i+1} - x_{i+1}|$$

$$= |x'_i + 4k_1 - x_i| + |x'_{i+1} + 2k_2 - x_{i+1}|$$

$$= |4k_1 + r_1| + |2k_2 + r_2| \quad (4)$$

In the only event that data readjusting mechanism is applied under Case #1 and Case #2, according to the principle of embedding mechanism, each pixel-couple has only one pixel to be added or reduced by 1, whereby the r_1 and r_2 conform to $r_1, r_2 \in \{0, -1, +1\}$ and $|r_1| + |r_2| = 1$. The absolute difference of pixel couple changed in data readjusting mechanism is no less than T on the condition that r_1 and r_2 conform to $|r_1| + |r_2| \neq 0$. The following process of proof for k_1 and k_2 shall be represented by such two processes of proof as $x'_i - x'_{i+1} = T - 1$ and $x'_{i+1} - x'_i = T - 1$.

(I) Where $x'_i - x'_{i+1} = T - 1$: $x'_i - x'_{i+1} = T - 1$ and $x'_{i+1} \geq 2$ only occurs under $x'_i = x_i - 1$ (Case #3) or $x'_{i+1} = x_{i+1} + 1$ (Case #2), so $r_1 = -1, r_2 = 0$ (Case #3) or $r_1 = 0, r_2 = 1$ (Case #2). Based on the formula (4)

and $|k_1| + |k_2| \neq 0$, in such two cases, $k_1=0$ and $k_2 = -1$. On the condition of $x'_i = x_i - 1$ (Case #3), although $k_2 = 1$ also conforms to the requirement of formula (4) under $r_1 = -1, r_2 = 0$ (Case #3), in order to conform to $x''_{i+1} - x'_i \geq T$, the case is $k_2 \neq 1$.

For the case of $x'_i - x'_{i+1} = T - 1$ and $x'_{i+1} < 2$, $x''_{i+1} = x'_{i+1} + 2k_2$, so $k_2 \neq 1$, which means that k_2 could only be 0 or 1. Based on formula (4) and $|k_1| + |k_2| \neq 0$, where $r_1 = -1, r_2 = 0$ (Case #3), if $k_2 = 0$ and $k_1 = 1$, the only and minimal of formula (4) will be 3, and the case is $x'_i - x'_{i+1} = T + 3$; if $k_2 = 1$ and $k_1=0$, the only and minimal of formula (4) will still be 3, but the $x'_i - x''_{i+1} = T - 3$ does not meet the preconditions of this algorithm. Therefore, the case is $k_1=1, k_2=0$ and $x'_i - x''_{i+1} = T + 3$. Where $r_1=0, r_2=1$ (Case #2), if $k_2=0$ and $k_1=\pm 1$, the only and minimal of formula (4) will be 5; if $k_1=1$, the case is $x''_i - x''_{i+1} = T + 3$ and if $k_1=-1$, the case is $x''_i - x''_{i+1} = T - 3$. Therefore, the case is $k_1 = 1$; if $k_2 = 1$ and $k_1=0$, the only and minimal of formula (4) will be 3 and the case is $x''_i - x''_{i+1} = T - 3$. Therefore, the final case is $k_1 = 1, k_2 = 0$ and $x'_i - x''_{i+1} = T + 3$.

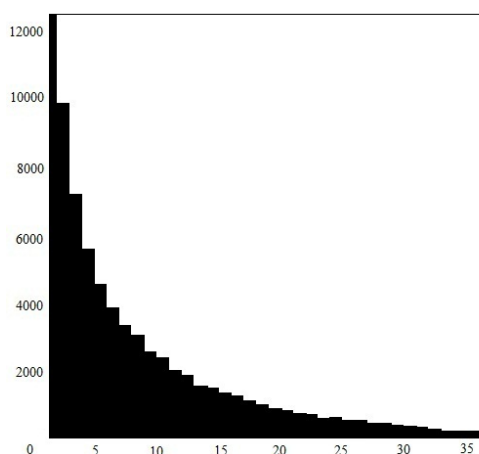
(II) Where $x_{i+1} - x_i = T - 1$: The case of $x'_{i+1} - x'_i = T - 1$ and $x'_{i+1} \leq 253$ only occurs under condition of $x'_i = x_i + 1$ (Case #4) or $x'_{i+1} = x_{i+1} - 1$ (Case #2). Therefore, the case is $r_1 = 1, r_2 = 0$ (Case #4) or $r_1 = 0, r_2 = -1$ (Case #2). Based on formula (4) and $|k_1| + |k_2| \neq 0$, in such two cases $k_1=0$ and $k_2=1$. In case of $x'_i = x_i + 1$ (Case #3), although the case of $r_1 = 1, r_2 = 0$ (Case #4) and $k_2 = -1$ also meets the requirements of formula (4), to meet $x''_{i+1} - x'_i \geq T$, $k_2 \neq -1$.

For the case of $x'_{i+1} - x'_i = T - 1$ and $x'_{i+1} > 253$, $x''_{i+1} = x'_{i+1} + 2k_2$, so $k_2 \neq 1$, which means that the k_2 can only be 0 or -1. Based on formula (4) and $|k_1| + |k_2| \neq 0$, where $r_1 = 1$ and $r_2 = 0$ (Case #4), if $k_2=0$ and $k_1 = -1$, the only and minimal value of formula (4) is 3 and the case is $x'_{i+1} - x'_i = T + 3$; if $k_2 = -1$ and $k_1=0$, the only and minimal value of formula (4) is 3 but the $x'_{i+1} - x'_i = T + 3$ does not conform to the preconditions of the algorithm. Therefore, the case is $k_1 = -1, k_2 = 0$ and $x'_{i+1} - x'_i = T + 3$. Where $r_1 = 0$ and $r_2 = -1$ (Case #2), if $k_2=0$ and $k_1 = \pm 1$, the only and minimal value of formula (4) is 5; if $k_1=1$, the case is $x''_{i+1} - x'_i = T - 3$ and if $k_1 = -1$, the case is $x''_{i+1} - x'_i = T + 3$. Therefore, the case $k_1 = -1$; if $k_2 = -1$ and $k_1 = 0$, the only and minimal value of formula (4) is 3, and the case is $x''_{i+1} - x'_i = T - 3$. Therefore the final case is $k_1 = -1, k_2 = 0$ and $x'_{i+1} - x'_i = T + 3$.

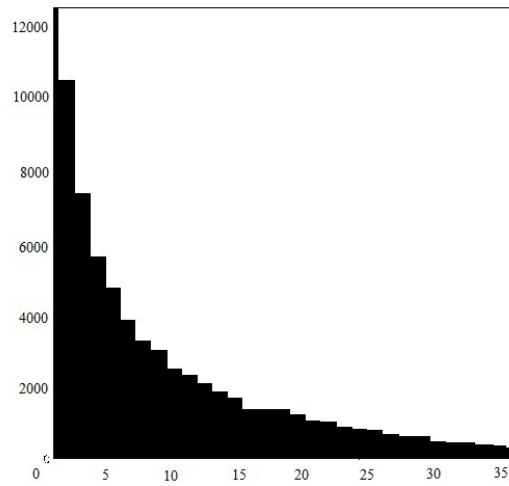
For all above, where $x'_i - x'_{i+1} = T - 1$ and $x'_{i+1} \geq 2$, $k_1 = 0, k_2 = -1$ and $|x'_i - x''_{i+1}| = T + 1$; where $x'_{i+1} - x'_i = T - 1$ and $x'_{i+1} < 253$, $k_1 = 0, k_2 = 1$ and $|x'_i - x''_{i+1}| = T + 1$; these are prevailing cases in EALMR, which bring significant statistical changes to stego images.

Through the analysis above, it can be seen that if the data readjusting mechanism in the EALMR makes effects, the number of pixel couples in the images, whose absolute difference is T , will change, which means that the absolute difference of some pixel couples will become $T+1$, such changing probability is up to 0.75. Hence, this algorithm respectively analyzes the horizon and vertical histograms of absolute difference of adjacent pixels for the purpose of EALMR detection. Fig. 1 and Fig. 2 show the original carrier image and the stego image after the information is embedded as well as its horizon and vertical histograms of absolute difference of adjacent pixels. It can be seen from Fig. 1 and Fig. 2 that, after the information is embedded through EALMR, the stego information is not such changed visually compared with the original carrier image, but there are obvious pulse distortions in the long tails of horizon and vertical histograms of absolute difference of adjacent pixels.

Therefore, for a given image A, if there is a pulse point found in its histograms of absolute difference of adjacent pixels, the image will be identified as a EA stego image; if there isn't, the image will be identified as a non-EA stego image.

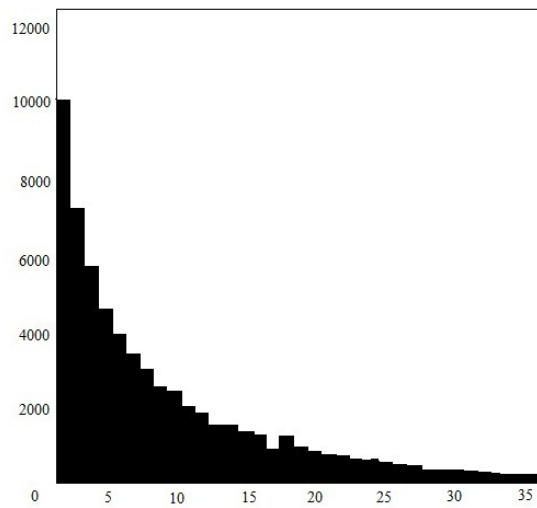


(a) The horizon histogram of the absolute difference of adjacent pixels

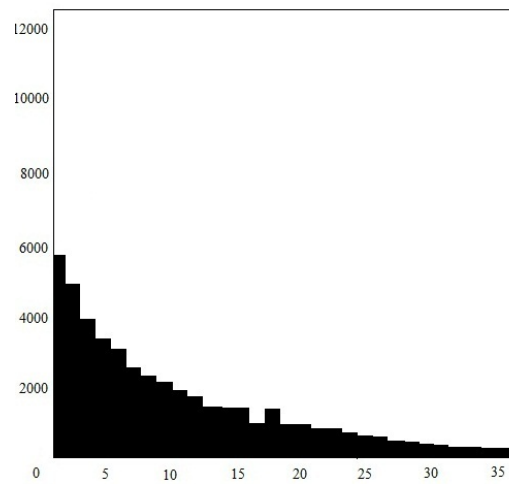


(b) The vertical histograms of the absolute difference of adjacent pixels.

Fig. 1: Original carrier image vegetable.



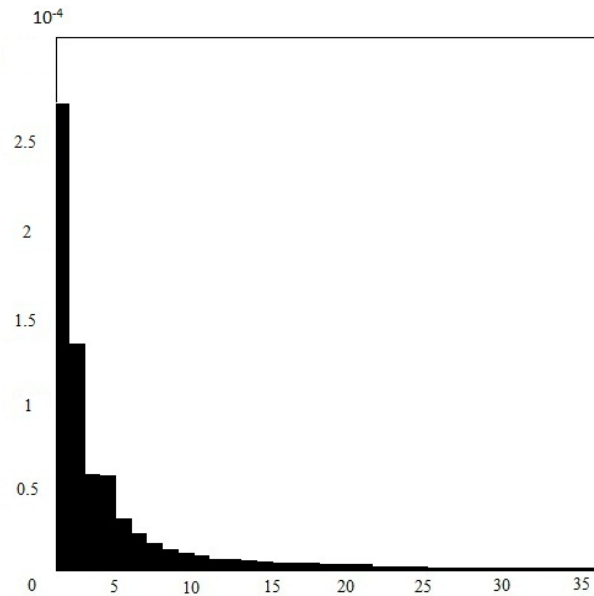
(a) The horizon histograms of the absolute difference of adjacent pixels.



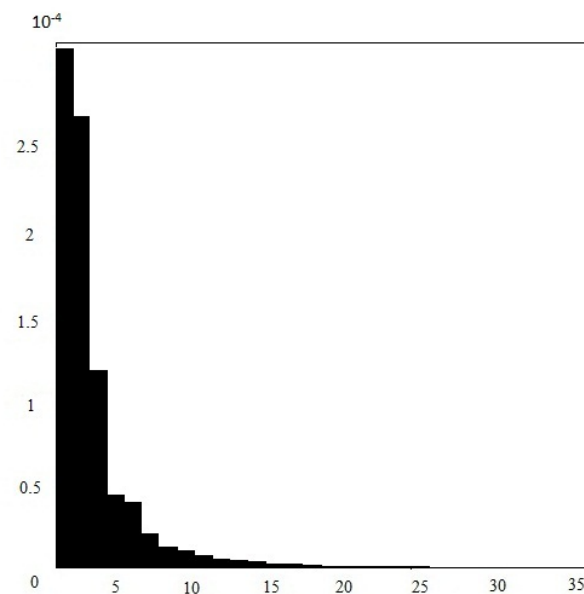
(b) The vertical histograms of the absolute difference of adjacent pixels

Fig. 2: EA stego image vegetable.

To further analyze Fig. 1 and Fig. 2, it is not hard to see that the distortions in Fig. 2(a) and Fig. 2(b) occur at 18 on the x ordinate, namely $T+1=18$, so it can be estimated that the threshold $T=17$ is used for embedding EA secret information of the Party regulations into such image. The proposed steganalysis algorithm allows not only to directly analyze whether the secret information is embedded into the image through EALMR but to estimate the threshold T . However, there is a kind of image, into which the information is embedded through EALMR, and the statistical properties of its horizontal and vertical histograms of absolute difference of adjacent pixels keep the same. Fig. 3 and Fig. 4 show the original carrier image that has such a special circumstance and the stego image after the information is embedded as well as its horizontal and vertical histograms of absolute difference of adjacent pixels.

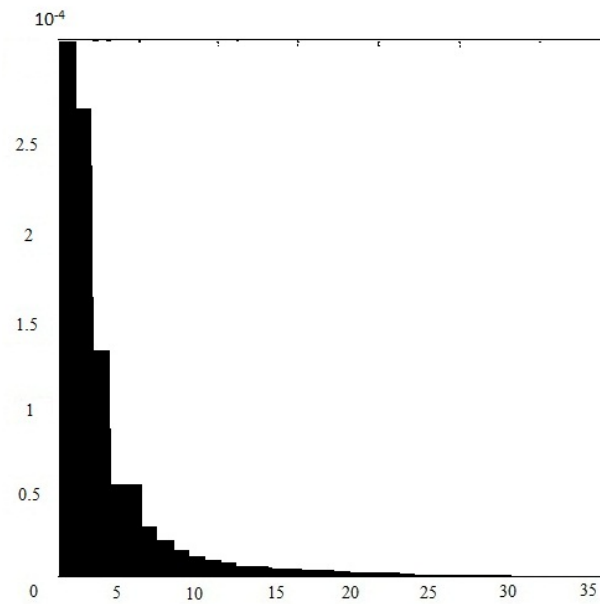


(a) The horizontal histograms of the absolute difference of adjacent pixels

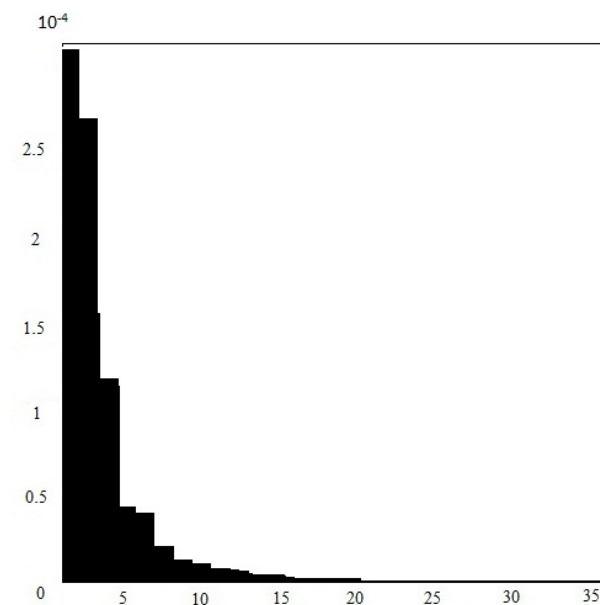


(b) The vertical histogram of the absolute difference of adjacent pixels

Fig. 3: Original carrier image flower.



(a) The horizontal histogram of the absolute difference of adjacent pixels



(b) The vertical histogram of the absolute difference of adjacent pixels

Fig. 4: EA stego image flower.

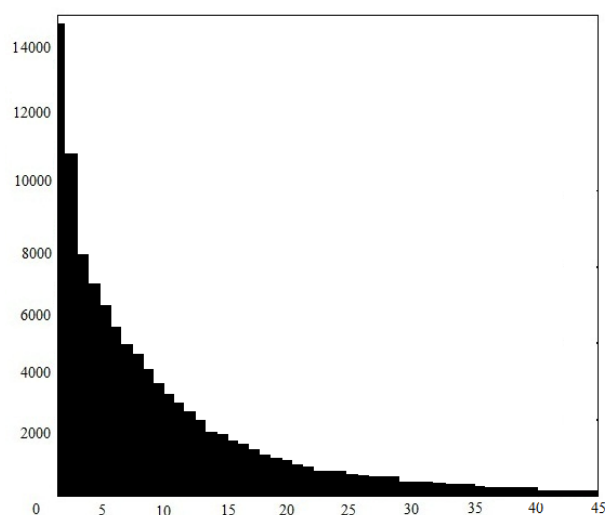
From Fig. 3 and Fig. 4, after the EA secret information of the Party regulations is embedded into the original image Flower, there is no obvious change both of histograms of absolute differences of horizontally and vertically adjacent pixels, neither the pulse distortion that should exist in the long tail. If these images are selected for EA embedding, the detection will fail.

RESULTS AND DISCUSSIONS

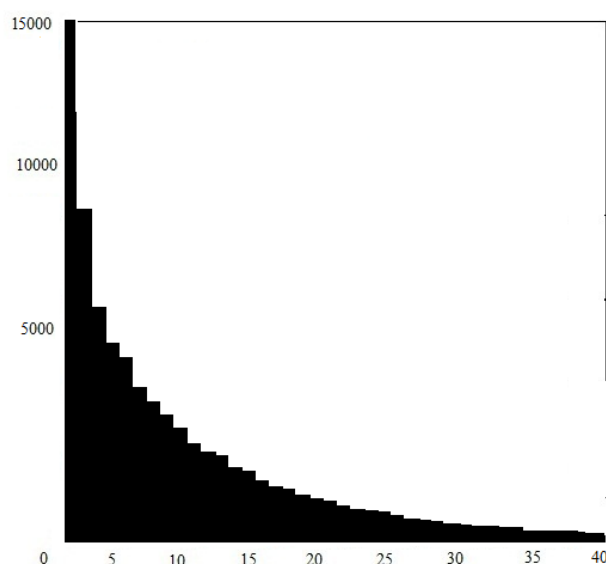
The image pool for experiments is BOSSbase ver.0.92, including 9,074 grey pgm images with resolution of 512x512. EALMR is applied for images by embedding 5%, 10%, 20%, 30%, 40% and 50% of secret information to respectively form stego image pools with different embedding rates. The statistical analysis can be directly carried out for images to be tested based on the analysis method of histogram of absolute difference of adjacent pixels, the test effect will be determined on the Average Accuracy. The higher the Average

Accuracy is, the better the test effect is. Five airspace steganalysis algorithms such as WAM, improved HCF, ALE, SPAM and SRM are used for comparison.

Fig.5 shows the original image of the tested image Piazza and its horizon and vertical histograms of the absolute difference of adjacent pixels; Fig.6 shows the EA stego image (imbedding rate 10%) and its horizon and vertical histograms of the absolute difference of adjacent pixels; Fig. 7 shows the EA stego image (imbedding rate 50%) and its horizon and vertical histograms of the absolute difference of adjacent pixels. Image Piazza has both smooth area and rich area and is typical, so it is selected to be the typical image to be tested. Tab.1 gives the test results of five steganalysis algorithms and the new proposed steganalysis algorithm based on the histogram of the absolute difference of adjacent pixels to EALMR.Tab 2 gives the accuracy rate of estimated threshold, which is calculated by the way that, for each EA stego image, if the estimated threshold is consistent with the actual threshold in image, the estimation is correct and the final accuracy rate the percentage of correct estimated images into the total images to be tested, subject to the average of results of ten repetitive experiments.

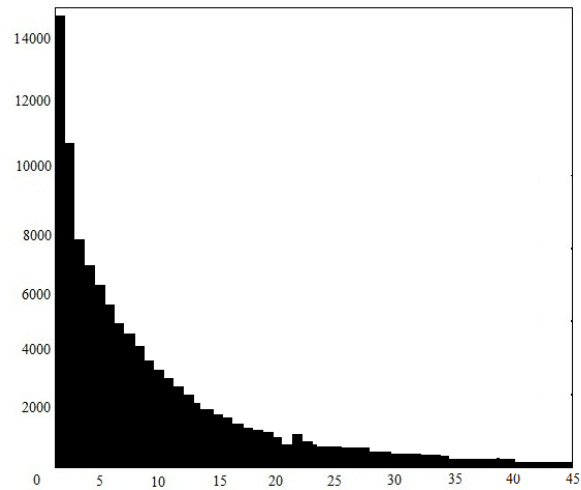


(a) Horizon histograms of the absolute difference of adjacent pixels

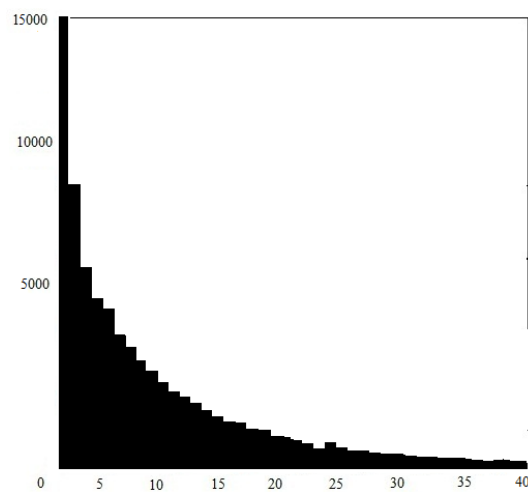


(b) Vertical histograms of the absolute difference of adjacent pixels

Fig. 5: Original image of the tested image Piazza.

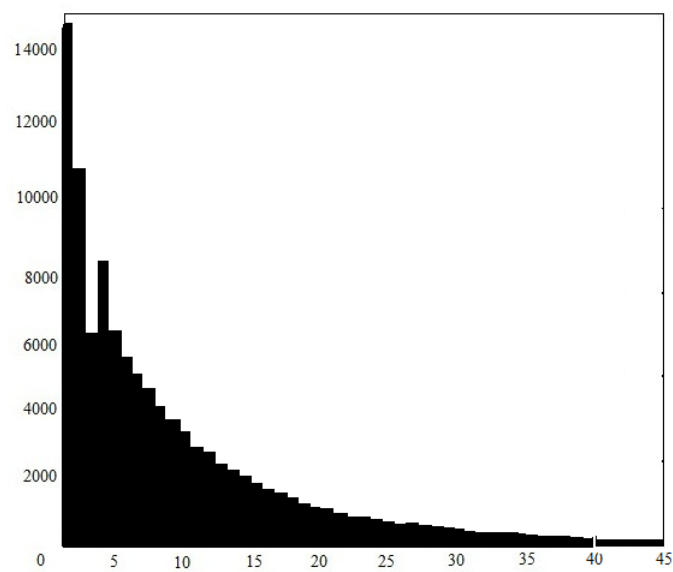


(a) Horizontal histograms of the absolute difference of adjacent pixels

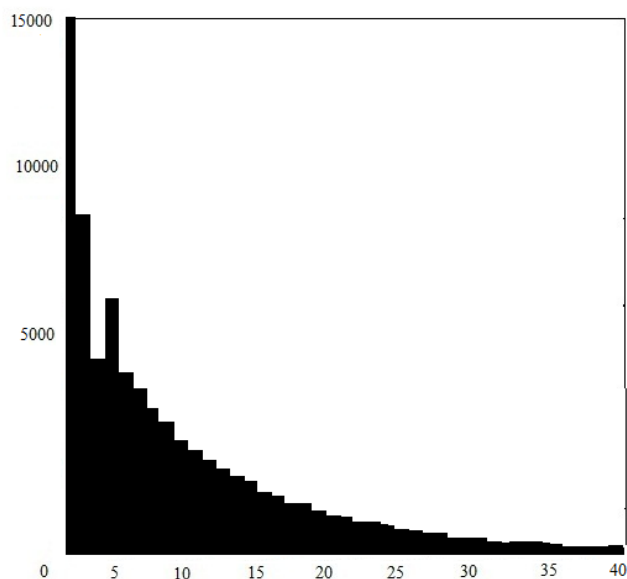


(b) Vertical histograms of the absolute difference of adjacent pixels

Fig. 6: EA stego image of the tested image Piazza (10%)



(a) Horizontal histograms of the absolute difference of adjacent pixels



(b) Vertical histograms of the absolute difference of adjacent pixels

Fig. 7: EA stego image of the tested image Piazza (50%).

From the places of the pulse distortion in Fig. (a) (b) and Fig. 7 (a) (b), it can be seen that where the embedding rate is 10% the threshold used for information embedding is $T = 24$; where the embedding rate is 50% the threshold used for information embedding is $T = 2$. It is visible that when the lower the embedding rate is the larger the threshold is, the generated EA stego image is safer; when the higher embedding rate is the smaller the threshold value is, the generated EA stego image is less safe. In addition, it is not hard to see from the experimental result figure that the pulse distortion height of stego image where the embedding rate is 50% is higher than that where the embedding rate is 10%. This is because, in the image Piazza, pixel-couple absolute difference is generally small, and minority of pixel couples have large absolute difference. Therefore, when the embedding rate significantly increases, the values of the threshold T will greatly decrease accordingly.

Table 1: Test results.

Embedding rate (%)	WAM method	HCF calibration method	ALE method	SPAM algorithm	SRM algorithm	Proposed algorithm
5	51.30%	49.78%	50.04%	51.41%	53.13%	97.50%
10	52.95%	51.40%	52.56%	53.36%	56.88%	98.10%
20	55.28%	54.59%	57.26%	56.82%	70.05%	98.25%
30	60.82%	56.32%	58.79%	61.76%	77.32%	98.45%
40	65.80%	63.28%	66.62%	69.95%	82.80%	99.05%
50	72.93%	65.63%	70.05%	75.52%	88.26%	99.40%

Table 2: Estimation accuracy

Embedding rate (%)	Estimation accuracy of threshold T
5	97.50%
10	98.10%
20	98.25%
30	98.45%
40	99.05%
50	99.40%

Compared with the result of the experiment in Tab. 1, it can be seen that the proposed analytical algorithm based on histogram of absolute difference of adjacent pixels can effectively detect EALMR, and has accuracy rate at least 97.50% when detecting stego image with low embedding rate. From Tab. 2, the estimation accuracy of threshold T is consistent with EALMR detection accuracy of this proposed algorithm in Tab. 1. This is because the detection principle of the proposed algorithm is to determine whether the image to be tested has information embedded through EALMR by judging whether there is pulse distortion at the long tail of histogram of absolute difference of adjacent pixels, and the place of the distortion is $T + 1$. Therefore, so as long as it can detect that the image to be tested is EA stego image, threshold T will then be estimated.

For further analysis with the results of the experiment, the reason why the proposed steganalysis algorithm has a higher detection rate on EALMR than other airspace steganalysis algorithms is that the steganalysis

algorithm is based on EALMR itself as a starting point, aims to the influence from information embedding mechanism and data readjusting mechanism, which is the pulse distortion of long tail of histogram of absolute difference of adjacent pixels to make detection and analysis.

Conclusion:

This paper proposed Steganalysis algorithm based on histograms of the absolute difference of adjacent pixels to detect EALMR. This algorithm firstly analyzes the impact of information embedding mechanism and data readjusting mechanism in the EALMR on stego image, indicates that such influence brings obvious pulse distortion to the long tail of histogram of absolute difference of adjacent pixel of the stego image, and provides an effective analysis algorithm to detect EALMR. The corresponding experiment is made in view of the proposed algorithm, and the experiment results are analyzed. The result verifies the accuracy of this algorithm to be used to detect EALMR and better detection effect of this algorithm with low embedding rate than other steganalysis algorithms. In addition, based on further analysis, with this algorithm, the threshold T used when information is embedded into stego image can be predicted.

REFERENCES

- Bender, W., D. Gruhl, N. Morimoto and A. Lu, 1996. Techniques for Data Hiding. IBM System Journal, 35(3-4): 313-336.
- Cancelli, G., G. Doerr, J. Cox, M. Barni, 2008. Detection of ± 1 LSB Steganography Based on the Amplitude of Histogram Local Extrema. In 15th IEEE International Conference on Image Processing, ICIP, pp: 1288-1291.
- Chandramouli, R., M. Kharrazi and N. Memon, 2003. Image Steganography and Steganalysis: Concepts and Practice. Proceedings of 2nd International Workshop on Digital forensics and Watermarking, South Korea, 2939: 35-49.
- Fillatre, L., 2012. Adaptive Steganalysis of Least Significant Bit Replacement in Grayscale Natural Images. IEEE Transactions on Signal Processing, 60(2): 556-569.
- Filler, T., J. Fridrich and J. Judas, 2010. Minimizing Embedding Impact in Steganography Using Trellis-Coded Quantization. In Proceedings SPIE, E, Media Forensics and Security XII, San Jose, pp: 1-14.
- Filler, T., J. Judas and J. Fridrich, 2011. Minimizing Additive Distortion in Steganography using Syndrome-Trellis Codes. IEEE Transactions on Information Forensics and Security, 6(3): 920-935.
- Fridrich, J. and J. Kodovsky, 2012. Rich Models for Steganalysis of Digital Images. IEEE Transactions on Information Forensics and Security, 7(3): 868-882.
- Fridrich, J. and M. Goljan, 2002. Practical Steganalysis of Digital Images-State of the Art. In Security and Watermarking of Multimedia Contents IV, Proceedings of SPIE, pp: 1-13.
- Fridrich, J., J. Kodovsky, V. Holub and M. Goljan, 2011. Steganalysis of Content-adaptive Steganography in Spatial Domain. In Proceedings of the 13th International Conference on Information Hiding, Berlin, Heidelberg, pp: 102-117.
- Fridrich, J., J. Kodovsky, V. Holub and M. Goljan, 2011. Breaking HUGO: The Process Discovery. In Proceedings of the 13th International Conference on Information Hiding, pp: 85-101.
- Fridrich, J., M. Goljan, R. Du, 2001. Detecting LSB Steganography in Color and Gray-Scale Images. Magazine of IEEE Multimedia, Special Issue on Security, pp: 22-28.
- Goljan, M., J. Fridrich and T. Holotyak, 2006. New Blind Steganalysis and Its Implications. In Proceedings of the SPIE, Security, Steganography, and Watermarking of Multimedia Contents, VI: 1-13.
- Gul, G. and F. Kurugollu, 2011. A New Methodology in Steganalysis: Breaking Highly Undetectable Steganography (HUGO). In Proceedings of the 13th International Conference on Information Hiding, Berlin, Heidelberg, pp: 71-84.
- Harmsen, J. and W. Pearlman, 2003. Steganalysis of Additive-noise Modelable Information Hiding. In Proc. SPIE, Security Watermarking Multimedia Contents, 5020: 131-142.
- Ker, A., 2005. Steganalysis of LSB Matching in Grayscale Images. IEEE Signal Processing Letters, 12(6): 441-444.
- Luo, W., F. Huang and J. Huang, 2010. Edge Adaptive Image Steganography Based on LSB Matching Revisited. IEEE Transactions on Information Forensics and Security, 5(2): 201-214.
- Pevny, T., T. Bas and J. Fridrich, 2009. Steganalysis by Subtractive Pixel Adjacency Matrix. In Proceedings of the 11th ACM workshop on Multimedia and security, pp: 75-84.
- Pevny, T., T. Filler and P. Bas, 2010. Using High-dimensional Image Models to Perform Highly Undetectable Steganography. In Proceedings of the 12th International Conference on Information Hiding, pp: 161-177.
- Schottle, P., S. Kor and R. Bohme, 2012. Weighted Stego-image Steganalysis for Naive Content-adaptive Embedding. In WIFS, pp: 193-198.

Sharp, T., 2001. An Implementation of Key-based Digital Signal Steganography. In Proceedings of the 4th International Workshop on Information Hiding, London, UK, pp: 13-26.

Westfeld, A. and A. Pfitzmann, 2000. Attacks on Steganographic Systems. In Information Hiding, Third International Workshop, Dresden, Germany, Proceedings, Lecture Notes in Computer Science, (1768): 61-76.

Zhang, J., I.J. Cox and G. Doerr, 2007. Steganalysis for LSB matching in images with high-frequency noise. In Proceedings of the IEEE Work-shop on Multimedia Signal Processing, pp: 385-388.